Korean J. Chem. Eng., 36(11), 1940-1947 (2019)
DOI: 10.1007/s11814-019-0388-6

pISSN: 0256-1115
eISSN: 1975-7220

Effect of emulsified polymer binders on the performance of activated carbon electrochemical double-layer capacitors

Seul Lee*,‡, Bolormaa Gendensuren*,‡, Boyeon Kim, Sangik Jeon**, Young-Hyun Cho***, Taewon Kim***, and Eun-Suok Oh*,†**

*School of Chemical Engineering, University of Ulsan, 93 Daehak-ro, Nam-gu, Ulsan 44610, Korea
**Solution Advanced Technology Co. Ltd., Siheung-si, Gyeonggi-do, Korea
***Ulsan Technopark, 15 Jongga-ro, Jung-gu, Ulsan 44412, Korea
(*Received 2 July 2019 • accepted 10 September 2019*)

Abstract−The electrochemical properties of two water-emulsified polymers, styrene-butadiene rubber, and polytetrafluoroethylene, on activated carbon electrochemical capacitors were systematically compared. All electrodes were fabricated with different ratios of styrene-butadiene rubber and polytetrafluoroethylene: 4 : 0, 3 : 1, 2 : 2, and 1 : 3. A good dispersion of styrene-butadiene rubber nanoparticles maintains mesopores in activated carbon, whereas an increase in polytetrafluoroethylene binder content in the electrodes reduces mesoporous surface area significantly due to the lump polytetrafluoroethylene structure coagulated by smashed particles in water. The relatively strong adhesion of the styrene-butadiene rubber binder also leads to better cyclability for extremely long cycles and the rate capability with various current densities at room temperature. At a high temperature of 60 °C, however, the electrodes containing polytetrafluoroethylene binder showed comparable high specific capacitance due to the high thermal stability of polytetrafluoroethylene.

Keywords: Electrochemical Double-layer Capacitor, Emulsified Binder, Styrene-butadiene Rubber, Polytetrafluoroethylene, Activated Carbon

INTRODUCTION

Unlike secondary batteries, which perform reversible electrochemical reactions, electrochemical double-layer capacitors (EDLC), also known as super- or ultra-capacitors, show repeated ion absorption/desorption in the electrical double-layer during their charge/discharge processes. This non-faradaic mechanism makes the EDLC a fascinating energy storage device required for rapid charge/discharge with extremely long-lasting cycles (>500,000), even though the energy density is considerably lower than that of lithium ion batteries (LIB). Therefore, the EDLC has been used in a variety of applications, including the energy sources for small electronics and power back-up systems for mobile electronics, electric vehicles, and energy storage systems (ESS).

Activated carbon has been the main active material in EDLC electrodes owing to its enormous specific surface area, excellent stability, and low cost. Activated carbon is usually mixed with additives, such as a conducting material and polymer binder, in either water or organic solvents during the manufacture of the electrode. These additives are required to provide an electrical network in the electrode for electrons to move freely. On the other hand, the polymer binder inevitably blocks some portion of the pores of the activated carbon, ultimately leading to capacity loss of EDLCs. Thus far, considerable research has been conducted on the active material and electrolyte of EDLCs. On the other hand, there has been little interest in the polymer binder of EDLC electrodes.

As a representative organic-soluble binder, a highly nonreactive thermoplastic, polyvinylidene fluoride (PVdF), is mostly used for EDLCs owing to its excellent chemical and electrochemical resistance, good thermal and mechanical stability, and suitable rheological properties with carbon materials [1,2]. On the other hand, its weak hydrogen bonding necessitates a large PVdF content in the electrode, causing a decrease in both the energy and power densities of the EDLCs [3]. More seriously, an environmentally unfriendly n-methyl-2-pyrrolidone (NMP) solvent is used during the electrode manufacturing process. Another fluoropolymer, polytetrafluoroethylene (PTFE), was also used as a binder for carbon EDLCs [4,5]. Unlike PVdF, up to 60 wt% PTFE can be dispersed in water, which makes it possible to manufacture an electrode without an organic solvent. Abbas et al. [5] reported that all of the pores in activated carbon were affected by the binder, and that the PTFE resulted in less pore blockage than the PVdF. Such a difference in the electrode porosity due to the pore blocking of binders contributed to the superior electrochemical performance of PTFE-containing EDLCs compared to PVdF-containing EDLCs. Nevertheless, the insufficient adhesion capability of PTFE, which is even worse than that of PVdF, is unfavorable to extremely long-lasting cycles of EDLCs [6]. The strong hydrophobicity of PTFE also seriously interferes with aqueous electrolyte wetting, even though this can be improved by adding a small amount of polyvinylpyrrolidone (PVP) to the PTFE dispersion [7]. On the other hand, a few studies reported that non-

†To whom correspondence should be addressed.
E-mail: esoh1@ulsan.ac.kr
‡Equally contributed to this work.

toxic and water-soluble PVP can be used as the sole binder for supercapacitors depending on the organic electrolyte [8,9].

Typical conjugated polymers, such as polypyrrole, polyaniline, and poly(3,4-ethylenedioxythiophene), have often been applied to supercapacitors to improve the electrical conductivity of the binder and thus the electrodes [10-12]. Unfortunately, these conducting polymers could not maintain the mechanical integrity of the electrodes after long-term cycling, which is an indispensable characteristic of the polymer binder [3].

Therefore, many commercial capacitor industries use eco-friendly and adhesive polymer materials as a binder, e.g., styrene-butadiene rubber (SBR) and carboxymethyl cellulose (CMC). Indeed, these have been adopted successfully to lithium-ion battery anodes because the combination of the two polymers has good adhesion, high flexibility, and sufficient electrochemical stability without environmental issues in the electrode manufacturing process [13,14]. Some capacitor industries also use water-dispersed PTFE as the third component of the binder combination. Despite the advantages of water-based binders, there has been no systematic study on the use of the binders for carbon EDLCs. The present study examined the effects of the two water-dispersed (or emulsified) polymer binders, SBR and PTFE, on the electrochemical performance of activated carbon EDLCs. The SBR:PTFE ratio varied in the electrodes, whereas the amount of CMC used as a thickening agent for the electrode slurry was fixed. The following physical and electrochemical characterization tools were adopted: field emission scanning electron microscopy (FE-SEM), transmission electron microscopy (TEM), thermogravimetric analysis (TGA), differential scanning calorimetry (DSC), Brunauer-Emmett-Teller (BET) analysis, electrochemical impedance spectroscopy (EIS), cyclic voltammetry (CV), and cyclic and rate performance tests.

EXPERIMENT

1. Fabrication of Electrodes and Cells

High surface area activated carbon (YP-50F, Kuraray Chemical Co. Ltd., Japan) was mixed with super-P (Phoenix Materials Co. Ltd., South Korea) as a conducting agent and polymer binder in a homogenizer. Their percentages were 85 wt% for activated carbon, 8 wt% for super-P, and 7 wt% for the binders, respectively. As binder materials, two water-dispersed polymers, SBR and PTFE, were used with a highly viscous CMC solution as a thickening agent of the electrode slurry. These are commercially graded binder materials for battery applications. The content of CMC was fixed with 2 wt%, whereas the total amounts of SBR and PTFE were 5 wt to the SBR : PTFE ratio: 4 : 0, 3 : 1, 2 : 2, and 1 : 3. The sample using only PTFE (SBR : PTFE=0 : 4) was excluded because of its very weak adhesion to the electrodes. The mixed slurry was cast on commercially available etched aluminum foil and dried in a convection oven at 60 °C. The mass loading of the electrodes was approximately 5 mg cm^{-2} and their thickness was approximately 115 μm. Subsequently, the electrodes were placed overnight in a vacuum oven at 80 °C for complete moisture removal before being assembled to EDLCs. The 2032-coin types of cells were assembled in an argon-filled glove box using 1 M tetraethylammonium tetrafluoroborate (TEABF4) in acetonitrile (AcN) as the electrolyte.

2. Physical Characterization

The adhesion of the electrode was confirmed by the 180° peel strength of a 2-cm wide electrode strip using a texture analyzer (TA-PLUS, Lloyds Instruments Ltd.). The morphology of the electrode surface and the water-dispersed polymers was examined by FE-SEM (JEOL JSM 6500F) and biological TEM (H-7500, HITACHI Ltd.). The thermal stability of the water-dispersed polymers was observed by TGA (Q50 TA instruments). The temperature ranged from 25 °C to 800 °C with a ramping rate of 10 °C min^{-1} and the nitrogen sample gas flowed at a rate of 60 ml min^{-1}. DSC (Q20, TA Instruments) was also performed under a nitrogen atmosphere between −40 °C and 90 °C at a heating/cooling rate of 10 °C min^{-1}. The BET method was used to determine how much the additives, including the binder materials, block the surface area of the active materials. The specific surface area, pore size, pore volume, and pore distribution of the electrodes were analyzed by nitrogen adsorption/desorption at −196 °C using a Micromeritics ASAP 2020 (Micromeritics Instrument Co.) adsorption analyzer. The pore size distribution of the samples was analyzed using the Barrett-Joyner-Halenda (BJH) method. The contact angles of an electrolyte drop (1M TEABF4 in AcN) on thin binder films were measured as a function of time using a video-connected device (Theta Lite 100, KSV Instrument Ltd.) to examine the wettability of binders. The ionic conductivity of thin binder films was also measured through the EIS experiment of the film placed between two stainless-steel disk electrodes [15]. The binder film was fabricated using a mixture of emulsified SBR or PTFE and CMC thickening agent. The emulsified polymer to CMC ratio was 5 : 2 in weight, which was identical to the binder ratio of the electrode. A small amount of glycerol of 0.1 weight ratio was also added as a plasticizer of the binder film. For comparison, the ionic conductivity of the electrolyte was also measured using a conductivity meter (S230-K, Mettler-Toledo).

3. Electrochemical Characterization

For the first five cycles, the EDLC cells were charged galvanostatically to 2.7 V and maintained at that voltage for 30 min. They were then discharged to 0.1 V and maintained at that voltage for 30 min. The electrochemical performance of the coin cells was measured by charge/discharge between 2.7 V and 1.35 V in constant current mode at 10 mA F^{-1} for prolonged cycles in a battery cycle system (PNE solution Co., Korea). For rate capability mode, various current densities of 1, 5, 10, and 50 mA cm^{-2} were applied to the cells at room temperature. EIS (VSP, Biologic Science Instruments) was performed within the frequency range of 10^{-3} to 10^{6} Hz at room temperature. Using the same apparatus, CV of the EDLCs was also conducted at different scan rates of 5, 20, 50, and 100 mV s^{-1}.

RESULTS AND DISCUSSION

A polymer binder can improve the performance of EDLCs in a variety of ways. In particular, the strong adhesion, as an essential condition of the binder, can reduce the binder content needed in the electrodes, ultimately leading to an increase in both the energy and power densities. Moreover, it helps prevent cracks in the electrodes and delamination of the electrodes from the current collectors, which usually appears in long-lasting cycles. Electrode adhesion

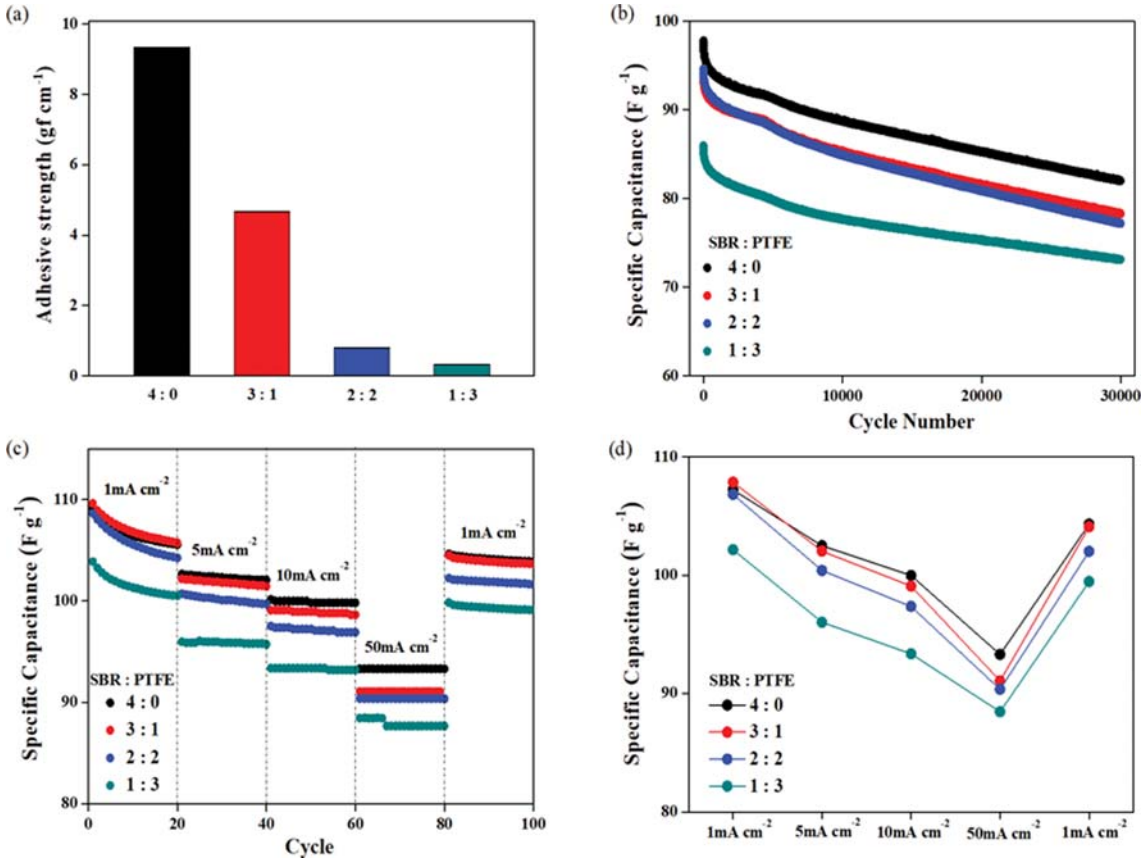

Fig. 1. (a) Adhesion strength of the electrodes measured by the 180° peel strength. (b) Cyclic performance of the EDLC cells containing different SBR/PTFE binder ratios. (c) Rate capability tests of the EDLC cells. The applied constant current densities were 1, 5, 10, and 50 mA cm^{-2}; each was maintained for 20 cycles. The current was returned to 1 mA cm^{-2} for the last 20 cycles. (d) Electrode specific capacitances calculated from the fifth cycle of each current density.

according to the different SBR/PTFE ratios was determined using the 180° peel strength and is illustrated in Fig. 1(a). As expected, the electrodes containing relatively large amounts of PTFE showed lower adhesion strength because of weak hydrogen bonds of PTFE with the hydrogen neighbors in the active materials. In particular, the sole PTFE binder (0 : 4 SBR : PTFE sample) failed to form a stable electrode on the current collector. In contrast, the electrode containing only SBR (4 : 0 sample) had relatively high adhesion. Therefore, it may be possible to decrease the SBR binder content to increase the energy density of the EDLCs.

For an EDLC cell composed of two symmetric electrodes arranged in series, the capacitance of the cell is simply half that of each electrode and can be measured by galvanostatic charge/discharge processes as follows:

$$C_{cell} = \frac{C_{elec}}{2} = \frac{I}{dV/dt} \quad (1)$$

where the capacitances of cell and electrode are denoted as C_{cell} and $C_{electrode}$, respectively. A constant current, I=10 mA F^{-1}, which is recommended for power application by the International Electrotechnical Commission (IEC) standard, was used to measure the time derivative of the voltage [dV/dt]. In addition, the specific (or gravimetric) capacitance (F g^{-1}) of an electrode was calculated using the mass of active materials in the electrode so that

$$C_{sp,\,elec} = \frac{C_{elec}}{m_{elec}} = \frac{2C_{cell}}{m_{cell}/2} = 4C_{sp,\,cell} \quad (2)$$

In Fig. 1(b), the cycling performance of the EDLCs containing different SBR/PTFE binder ratios is compared with their electrode-specific capacitance. Regardless of the binder ratios, there occurs main capacitance loss within the first hundred cycles. These must be caused by the removal of some functional groups in the activated carbon and the disappearance of pseudo-capacitance during the cycles [16,17]. The electrode composed of only the SBR binder showed higher initial and cyclic capacitances within 30,000 cycles than the other PTFE-containing electrodes. An analysis of the cycling stability with a gradual decrease in specific capacitance revealed the SBR : PTFE=2 : 2 sample to exhibit slightly poorer cycling stability than the 4 : 0 and 3 : 1 samples, but the difference was not significant. This may be due to a decrease in the adhesion strength with increasing PTFE binder content, as shown in Fig. 1(a). Therefore, the adoption of stronger binding systems for extremely long-cycled EDLCs would be favorable. The rate capability of the EDLCs was also performed with a current density ranging from 1 mA cm^{-2} to 50 mA cm^{-2}, and the results are shown in Fig. 1(c), (d). As expected from the result in Fig. 1(b), the cyclic capacitance of the 1 : 3 sam-

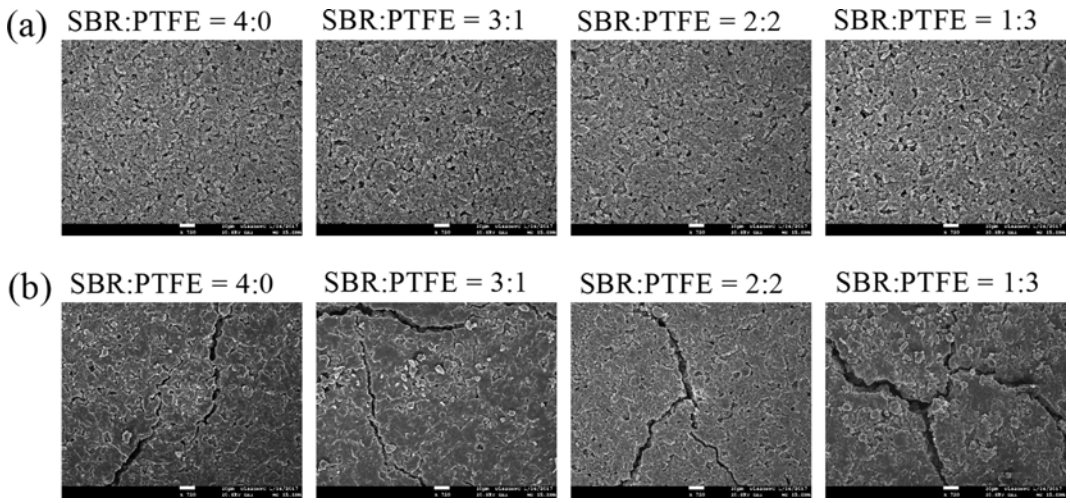

Fig. 2. FE-SEM images of the electrodes containing different SBR/PTFE binder ratios. (a) fresh electrodes and (b) 30,000-cycled electrodes.

ple was clearly inferior to the other three samples. Of the three, the 4 : 0 sample showed larger capacitance at all current densities and more importantly, showed a smaller decrease in capacitance with increasing current density. The 3 : 1 sample also showed a slightly better result than the 2 : 2 samples, but both samples were relatively worse at a high current charge/discharge of 50 mA cm^{-2}. Similar to long-lasting EDLCs, the EDLC cells achieving a high power current also require a strong adhesive binder to minimize the damage caused by the high currents.

This difference in electrode adhesion (Fig. 1(a)) affects the morphology of the cycled electrodes. FE-SEM was carried out over the fresh electrodes and 30,000-cycled electrodes obtained from the cyclic tests in Fig. 1(b), and the result is displayed in Fig. 2. The surface of the fresh electrodes became less porous as the PTFE content was increased. Compared to the fresh electrodes, the cycled electrodes contained small cracks, crevices, and obscure boundaries among the materials. When the electrolyte permeated into the porous active materials and the charge/discharge process was performed repeatedly, the physical structure of the active material changed and was even destroyed by a variety of mechanisms [18]. Strong adhesion helps minimize such a detrimental change during long cycles. The SBR : PTFE=4 : 0 sample has the highest adhesion force so that the electrode had the fewest cracks and crevices. In contrast, the electrode composed of the SBR : PTFE=1 : 3 binder showed severe deep crevices after 30,000 long cycles, even though no delamination of the electrode occurred.

As mentioned in the introduction, one of the main advantages of the PTFE binder is less pore blocking of activated carbon, which can lead to an increase in capacitance compared to the conventional PVdF binder [5]. The change in the electrode porosity due to the use of a polymer binder has been suggested as the origin of the change in the electrochemical performance, including high voltage floating and leakage current. BET measurements were taken to determine how the surface area and porosity of the activated carbon, having an enormous specific area because of the uncountable micropores (<2 nm in diameter), were affected by the ratio of the emulsified binders. Table 1 lists the pore size distribution of Fig. 3(a).

Table 1. BET surface area and total pore volume of activated carbon and electrodes containing different ratios of the binders

SBR : PTFE	S_{BET} [$m^2 g^{-1}$]	S_{micro} [$m^2 g^{-1}$]	S_{meso} [$m^2 g^{-1}$]	V_{total} [$cm^3 g^{-1}$]
YP - 50F	1701	1463	238	0.752
4 : 0	1432	1181	251	0.625
3 : 1	1427	1269	158	0.613
2 : 2	1387	1282	105	0.587
1 : 3	1344	1259	84	0.545

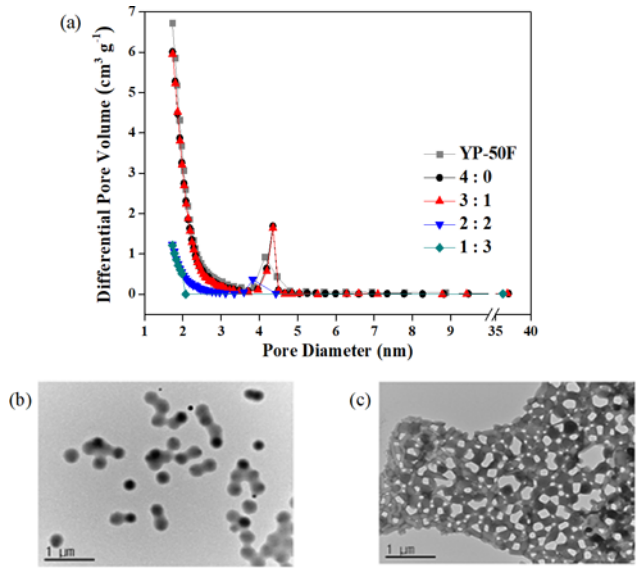

Fig. 3. (a) Pore size distribution curves analyzed using the BJH method. (b) and (c) TEM images of the SBR and PTFE emulsions, respectively.

The BET surface area and pore volume of the activated carbon decreased dramatically in the electrodes due to the presence of binders. Both experienced a gradual decrease with a relative increase in

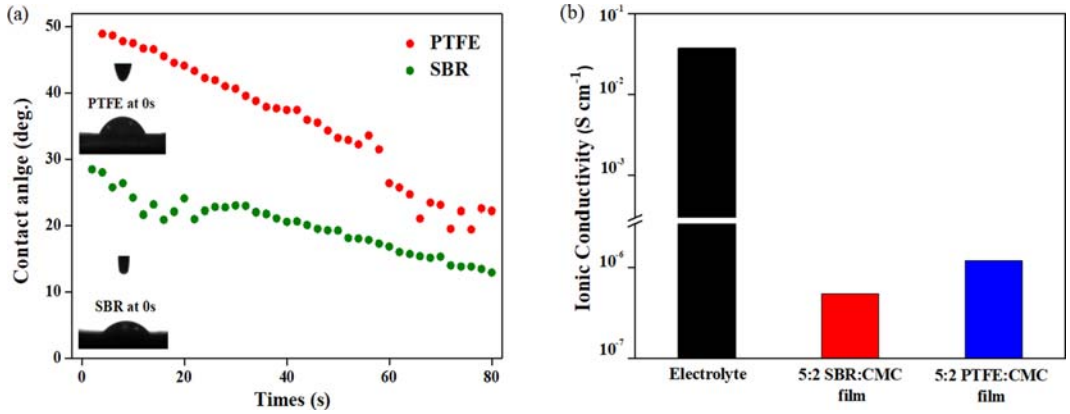

Fig. 4. (a) Contact angles of an electrolyte (1M TEABF4 in AcN) drop fallen on thin SBR and PTFE films. The insets show photographs of the initial contact angles taken at the instant when an electrolyte drop falls on the film. (b) Ionic conductivities of the electrolyte and the binder films, 5 : 2 SBR : CMC and 5 : 2 PTFE : CMC films.

the PTFE to SBR ratio, as expected from the SEM images of the fresh electrodes in Fig. 2(a). Considering the electrodes only, a noticeable variation in the BET surface area of the meso-pores (2-50 nm in diameter) was observed. The increase in PTFE content in the electrodes decreases the meso-pore surface area significantly. This must be related to the dispersion state of SBR or PTFE nanoparticles in water. TEM images of the SBR and PTFE emulsions in water (Fig. 3(b), (c)) showed that the SBR nanoparticles were well dispersed in water, whereas the PTFE particles formed a coagulated lump structure due to particles smashed in water. Such a large lump must block a larger number of meso-pores in activated carbon than the well-dispersed SBR nanoparticles. This is also confirmed in Fig. 3(a) by the decrease in pore volume corresponding to meso-pores with increasing PTFE contents.

Some studies have reported that it is difficult for the ions in the electrolyte to move in and out through very narrow micro-pores, whereas the ions moved relatively freely from bulk electrolyte solution to electrical double layers through the meso-pores [19,20]. Therefore, the large specific capacitance of the electrodes containing 4 : 0 or 3 : 1 in Fig. 1 can be attributed directly to less meso-pore blocking of the well-dispersed SBR nanoparticle binder.

The ion transport through the polymer binder is much slower than that through the electrolyte [21]. Nevertheless, it would be more favorable for the rapid charge/discharge of EDLCs if the ions move actively in the binder and electrolyte. The intrinsic characteristic of the binder for ion transport can be estimated using both the contact angle and the ionic conductivity of a thin binder film. As shown in Fig. 4(a), the initial contact angle of PTFE, which was measured when an electrolyte drop falls on the film, was higher than that of SBR. This indicates that PTFE has inferior electrolyte affinity compared to SBR, which must be due to the non-stick property of PTFE caused by its strong cohesive force originating from strong carbon-fluorine bonds. The difference in their contact angles became smaller and the contact angle of the SBR film reached an unmeasurable angle (θ<10°) after approximately 80 sec, whereas that of the PTFE films required more than 100 sec. This indicates that the SBR binder has an advantage on electrolyte wetting and perhaps ion transport.

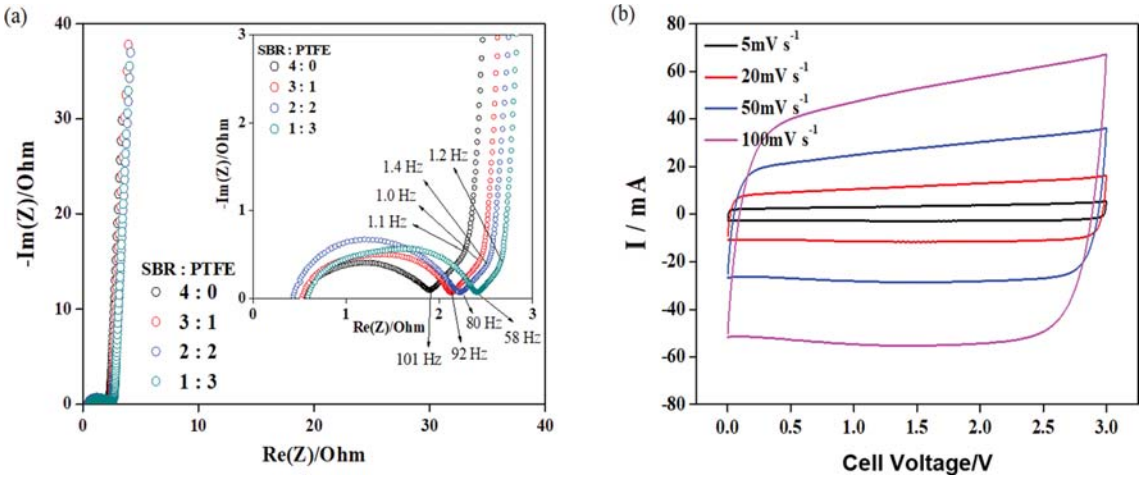

Fig. 5. (a) Nyquist plots of the 10,000 cycled EDLC cells with the frequency ranged from 10^{-2} to 10^{6} Hz at 0 V. (b) Cyclic voltammograms of the 4 : 0 SBR : PTFE EDLC over the voltage ranged from 0 V to 3 V with the different scan rates of 5, 20, 50 and 100 mV s^{-1}.

Fig. 4(b) presents the ionic conductivities of the electrolyte and the binder films. As expected, the electrolyte has significantly higher ionic conductivity of more than 3.5×10^{-2} S cm^{-1} compared to the binder films. The ionic conductivity of the 5 : 2 SBR : CMC and PTFE : CMC films was 5.11×10^{-7} and 1.18×10^{-6} S cm^{-1}, respectively. Therefore, the ion transport through the binder film is negligible compared to the ion transport through the electrolyte in the electrode. However, the emulsified binder still has an influence on the ion transport of electrode by altering some characteristics of the electrode such as electrolyte wetting and electrode morphology. The difference in ionic conduction over the electrodes containing different binder SBR : PTFE ratios will be also discussed through the EIS results.

To analyze the electrochemical characteristics of the EDLCs on the ratio of SBR/PTFE binders, EIS and CV were conducted on the EDLCs cycled for up to 10,000 charge/discharge processes at a current density of 10 mA F^{-1}; the results are in Fig. 5. Fig. 5(a) presents the impedance spectra of the cells. Three distinctive regions can be seen depending on the frequency in the Nyquist plot. The equivalent series resistance (ESR) at a very high frequency, which is the internal alternative current resistance, is generally determined from the first *x*-intercept of the Nyquist plot and represents the resistance from the electrolyte solution of the cells and the active materials of the electrodes [22,23]. Owing to the EDLC characteristics of the physical charge/discharge process, the ESRs of EDLCs were much lower than those of LIBs. The values obtained from the inset in Fig. 5(a) were 0.52 Ω for the SBR : PTFE=4 : 0 sample, 0.52 Ω for the 3 : 1 sample, 0.43 Ω for the 2 : 2 sample, and 0.59 Ω for the 1 : 3 sample. The semi-circles in the high frequency range indicate the magnitude of contact resistance, which is related to the interfacial resistance of the electrode/electrolyte and electrode/current collector [5]. Therefore, the second *x*-intercept of the Nyquist plot is the sum of ESR and the contact resistance and is in the order of 4 : 0<3 : 1<2 : 2<1 : 3. As explained previously from various experiments, the stronger adhesion of the SBR binder forms better contact between the activated carbon and current collector with less plugging of the original pores in the activated carbon and better electrolyte wetting. Such advantages of the SBR binder must contribute to the lower resistance in the EIS experiments.

The Warburg diffusion region has lower frequencies that continue to the knee frequency, the maximum frequency for the capacitive behavior of the EDLC, with a straight line having a 45° slope, implying the diffusion of ions in the pores. The Warburg region became increasingly prominent with increasing SBR content in the binder. Consistent with Table 1 and Fig. 3, this was attributed to the more porous structure in the electrode when the SBR/PTFE binder ratio increases. Nevertheless, the vertical lines at the very low frequencies show that the capacitive behavior of the activated carbon is well maintained regardless of the binder ratio.

Cyclic voltammetry (CV) was also carried out to examine the performance of EDLCs over a voltage window between 0 and 3 V with four different scan rates, 5, 20, 50, and 100 mV s^{-1}, as dis-

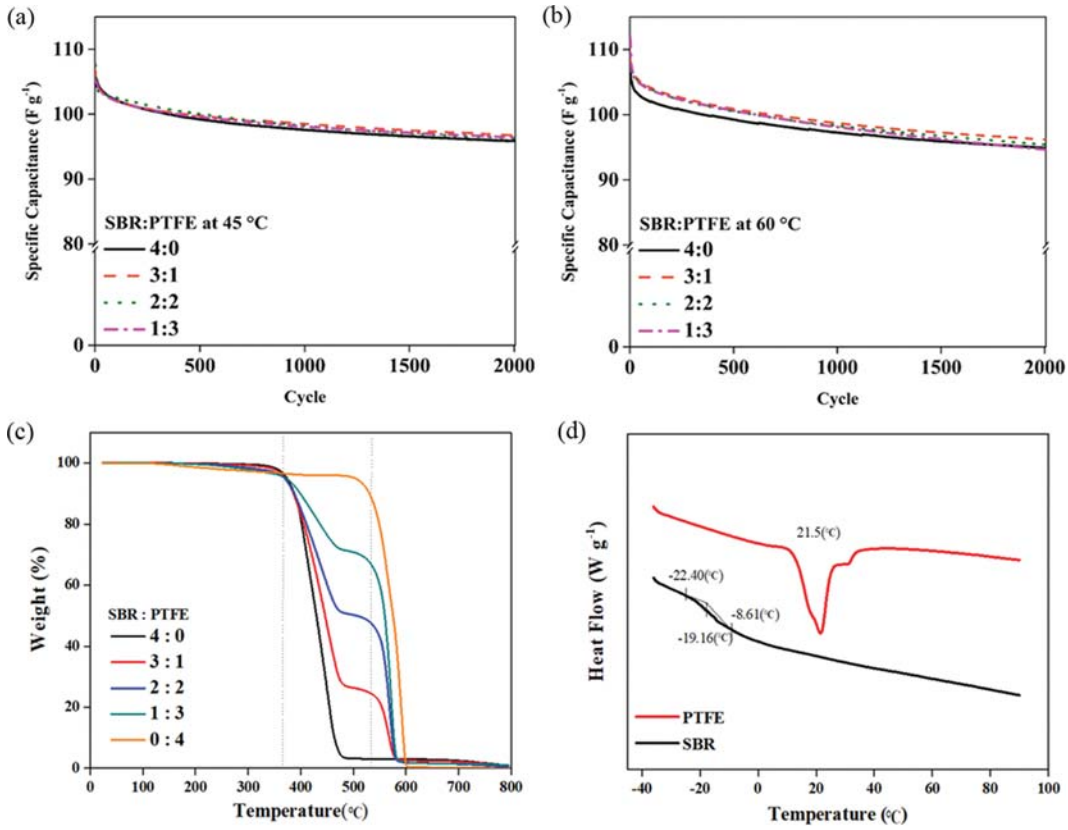

Fig. 6. Cyclic performance tests of the EDLC cells at the temperature of (a) 45 °C and (b) 60 °C. (c) TGA profiles of the binder samples from 25 °C to 800 °C. (d) DSC thermograms of the SBR and PTFE binders measured between −40 °C and 90 °C.

played in Fig. 5(b) for the SBR-containing EDLC only. The CV curves were barely distinguishable among the samples with different SBR/PTFE binder ratios (see Fig. S1 in the Supplementary Information.). All the samples showed rectangular shapes in their CV curves, indicating the typical capacitive behaviors of the EDLC cells. The lack of faradaic peaks shows that no apparent redox reactions caused by either SBR or PTFE polymer occur over the voltage range. The CV curves maintain rectangular shapes even with increasing scan rates, indicating good ion transfer in the AcN electrolyte solution of the SBR/PTFE-containing EDLCs [9].

EDLCs are sometimes exposed to severe conditions, such as higher or lower temperature environments. In the perspective of the polymer binder, the high temperature operation of EDLC cells should be examined rather than low temperature operation because the intrinsic binding capability of the polymer is affected more by an increasing temperature than by decreasing temperature from room temperature. The cyclic tests of the EDLCs were performed at high temperatures and the results obtained at 45 °C and 60 °C are shown in Fig. 6(a), (b). Unlike the result obtained at room temperature, which is shown in Fig. 1(b), the differences in specific capacitance among the samples were not significant. On the contrary, the 4 : 0 sample, which showed the highest cyclic capacitance at room temperature, has slightly lower cyclic capacitance at the highest temperature of 60 °C than the other samples. These imply that the temperature effect can differ according to the binder materials of the EDLCs.

To measure the thermal stability of SBR and PTFE, TGA was first carried out from 25 °C to 800 °C with a ramping rate of 10 °C min^{-1}, as shown in Fig. 6(c). The thermal degradation of SBR occurred around 380 °C, whereas PTFE began to degrade around 580 °C. SBR completely decomposed before 500 °C, but the PTFE remained even until 600 °C. The combined SBR/PTFE samples clearly showed two-step decompositions due to SBR and PTFE, respectively. Their weight loss was approximately proportional to the SBR/PTFE ratio. This TGA result shows that the PTFE binder must be more thermally stable than SBR. Furthermore, DSC was performed between −40 °C and 90 °C to determine what happens at high temperatures compared to that at room temperature. As shown in Fig. 6(d), the glass transition temperature of the SBR is approximately −19 °C. Hence, an increase in temperature transforms the SBR binder to a more rubbery state, leading to binder softening and swelling caused by larger amount of electrolyte uptake. Kovalenko et al. [21] reported that the substantial electrolyte uptake of binder films made the film significantly softer and led to worse electrochemical performance in LIBs, compared to stiff binders with no electrolyte uptake. Therefore, the increase in operating temperature must weaken the mechanical strength of the electrode containing SBR binder, which ultimately has a detrimental effect on its capacitance. In contrast, the DSC profile of PTFE shows only phase transformations below and above 20 °C among the phase II triclinic, phase IV hexagonal, and phase I pseudo-hexagonal crystals [24]. No glass transition of amorphous PTFE phases occurred over the temperature range. Indeed, PTFE generally reaches the degree of crystallinity of 60-80% and its glass transition and melting temperatures are approximately 115 °C and 330 °C, respectively [25,26]. This high thermal stability of PTFE is why the PTFE-containing electrodes are relatively less susceptible to the operating temperature as shown in Fig. 6(a), (b).

CONCLUSIONS

A systematic study on the water-based binder to activated carbon EDLCs was conducted for the first time by thoroughly investigating the effects of two emulsified polymers, SBR and PTFE, on the electrochemical performance of EDLCs. The EDLC electrodes were fabricated with different SBR : PTFE ratios: 4 : 0, 3 : 1, 2 : 2, and 1 : 3. Relatively strong adhesion of the SBR binder was found to be favorable for maintaining the cyclability of extremely long-cycled EDLCs and minimizing damage to the electrode, such as cracks and crevices caused by the high current density. The good dispersion of SBR nanoparticles in water had a much lesser effect on blocking the electroactive mesopores in activated carbon than the lump structure of PTFE dispersion. In addition, the sticky SBR binder had better electrolyte wetting than the non-stick PTFE caused by its strong cohesive force. Such advantages of the SBR binder helps lower the impedance resistance, ultimately leading to a higher specific capacitance when the SBR content in the binder increases. At relatively high temperature, however, there are little differences in cyclic capacitance among the samples. On the contrary, the 4 : 0 sample containing only SBR binder showed slightly lower cyclic capacitance at the highest temperature, 60 °C. This may be attributed to the inferior thermal stability of SBR compared to PTFE. The very low glass transition temperature of −19 °C of the SBR makes it more rubbery when the temperature is increased from room temperature to 60 °C, leading to electrodes with weakened mechanical strength and capacity loss. In contrast, the semi-crystalline PTFE maintained its state because its glass transition and melting temperatures are much higher than 60 °C.

In summary, the SBR is suitable as a binder for activated carbon EDLCs and PTFE can be added as a co-binder to the SBR for high temperature applications because of its good heat tolerance.

ACKNOWLEDGEMENTS

This study was financially supported by the Ministry of Trade, Industry, and Energy (MOTIE), Korea, under the "Regional Specialized Industry Development Program" supervised by the Korea Institute for Advancement of Technology (KIAT) (R0005989).

SUPPORTING INFORMATION

Additional information as noted in the text. This information is available via the Internet at http://www.springer.com/chemistry/journal/11814.

REFERENCES

1. K. Cendrowski, W. Kukulka, T. Kedzierski, S. Zhang and E. Mijowska, *Nanomaterials*, **8**, 1 (2018).
2. S. Parulekar, S. S. R. M. Holmukhe and P. B. Karandikar, *Int. J. Eng. Tech.*, **7**, 313 (2018).
3. Y. Gao, *Nanoscale Res. Lett.*, **12**, 387 (2017).

4. Y. Jiao, C. Qu, B. Zhao, Z. Liang, H. Chang, S. Kumar, R. Zou, M. Liu and K. S. Walton, *ACS Appl. Energy Mater.*, **2**, 5029 (2019).
5. Q. Abbas, D. Pajak, E. Frąckowiak and F. Béguin, *Electrochim. Acta*, **140**, 132 (2014).
6. K.-C. Tsay, L. Zhang and J. Zhang, *Electrochim. Acta*, **60**, 428 (2012).
7. S. Paul, K. S. Choi, D. J. Lee, S. Sudhagar and Y. S. Kang, *Electrochim. Acta*, **78**, 649 (2012).
8. M. Aslan, D. Weingarth, N. Jäckel, J. S. Atchison, I. Grobelsek and V. Presser, *J. Power Sources*, **266**, 374 (2014).
9. K. Lia, N. Maffei and E. Entchev, *J. Solid State Electrochem.*, **18**, 2535 (2014).
10. A. Eftekhari, L. Li and Y. Yang, *J. Power Sources*, **347**, 86 (2017).
11. Y. Han and L. Dai, *Macromol. Chem. Phys.*, **220**, 1800355 (2019).
12. Y. Wang, Y. Ding, X. Guo and G. Yu, *Nano Res.*, **12**, 1978 (2019).
13. F. Jeschull, D. Brandell, M. Wohlfahrt-Mehrens and M. Memm, *Energy Technol.*, **5**, 2108 (2017).
14. R. Wang, L. Feng, W. Yang, Y. Zhang, Y. Zhang, W. Bai, B. Liu, W. Zhang, Y. Chuan, Z. Zheng and H. Guan, *Nanoscale Res. Lett.*, **12**, 575 (2017).
15. S. Chauque, F. Y. Oliva, O. R. Cámara and R. M. Torresi, *J. Solid State Electrochem.*, **22**, 3589 (2018).
16. Y. Bai, R. B. Rakhi, W. Chen and H. N. Alshareef, *J. Power Sources*, **233**, 313 (2013).
17. H. Xu, B. Gao, H. Cao, X. Chen, L. Yu, K. Wu, L. Sun, X. Peng and J. Fu, *J. Nanomaterials*, **2014**, 1 (2014).
18. C. Saka, *J. Anal. Appl. Pyrolysis*, **95**, 21 (2012).
19. C.-M. Wang, C.-Y. Wen, Y.-C. Chen, J.-Y. Chang, C.-W. Ho, K.-S. Kao, W.-C. Shih, C.-M. Chiu and Y.-A. Shen, in *The 3rd International Conference on Industrial Application Engineering 2015 (ICIAE2015)* (2015).
20. W.-C. Liao, F.-S. Liao, C.-T. Tsai and Y.-P. Yang, *China Steel Technical Report*, **25**, 36 (2012).
21. I. Kovalenko, B. Zdyrko, A. Magasinski, B. Hertzberg, Z. Milicev, R. Burtovyy, I. Luzinov and G. Yushin, *Science*, **334**, 75 (2011).
22. X. Pan, G. Ren, M. N. F. Hoque, S. Bayne, K. Zhu and Z. Fan, *Adv. Mater. Interfaces*, **1**, 1400398 (2014).
23. H. Wu, Z. Lou, H. Yang and G. Shen, *Nanoscale*, **7**, 1921 (2015).
24. P. Zhao, N. Soin, K. Prashanthi, J. Chen, S. Dong, E. Zhou, Z. Zhu, A. A. Narasimulu, C. D. Montemagno, L. Yu and J. Luo, *ACS Appl. Mater. Interfaces*, **10**, 5880 (2018).
25. J. W. Nicholson, *The Chemistry of Polymers*, Royal Society of Chemistry (2012).
26. M. Conte, B. Pinedo and A. Igartua, *Tribol. Int.*, **74**, 1 (2014).

Supporting Information

Effect of emulsified polymer binders on the performance of activated carbon electrochemical double-layer capacitors

Seul Lee*,‡, Bolormaa Gendensuren*,‡, Boyeon Kim, Sangik Jeon**, Young-Hyun Cho***, Taewon Kim***, and Eun-Suok Oh*,†**

*School of Chemical Engineering, University of Ulsan, 93 Daehak-ro, Nam-gu, Ulsan 44610, Korea
**Solution Advanced Technology Co. Ltd., Siheung-si, Gyeonggi-do, Korea
***Ulsan Technopark, 15 Jongga-ro, Jung-gu, Ulsan 44412, Korea
(*Received 2 July 2019 • accepted 10 September 2019*)

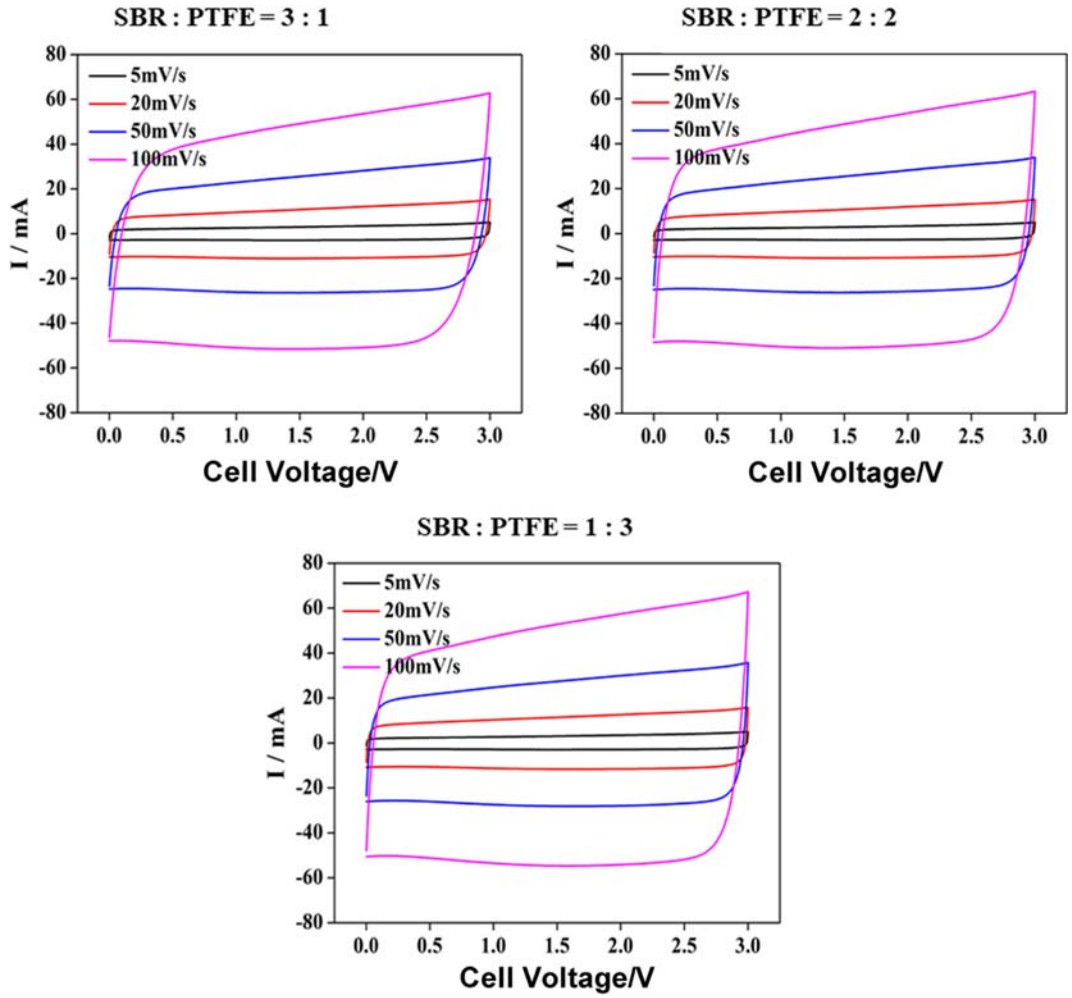

Fig. S1. Cyclic voltammograms of the 3 : 1, 2 : 2, and 1 : 3 SBR : PTFE EDLCs over the voltage ranged from 0 V to 3 V with the different scan rates of 5, 20, 50, and 100 mV s^{-1}.